Journal of Metals, Materials and Minerals, Vol. 29, No. 3, pp. 10-16, 2019

Enhanced corrosion resistance of hard steel wires produced by electrochemical cold drawing

Dong ZHAO[1], Feng YE[1], Yaakov B. UNIGOVSKI[2,*], Emmanuel M. GUTMAN[2], and Roni SHNECK[2]

[1] *State Key Laboratory for Advanced Metals and Materials, University of Science and Technology Beijing, 30 Xueyuan Road, Beijing 100083, China*
[2] *Department of Materials Engineering, Ben-Gurion University of the Negev, Beer-Sheva, 84105, Israel*

[*]**Corresponding author e-mail:** yakovun@bgu.ac.il

Received date:
13 February 2019
Revised date:
14 June 2019
Accepted date:
20 August 2019

Keywords:
FeSi6.5 steel
Electrochemical cold drawing
Anodic polarization
Corrosion resistance

Abstract

The corrosion resistance of AISI 1070 and FeSi6.5 steel wires produced by conventional cold drawing (CD) and electrochemical cold drawing (ECD) technologies were compared. The corrosion rate of steel wire FeSi6.5, obtained by the method of ECD, was lower than that of the wire obtained by the method of CD, while this difference for steel AISI 1070 was not pronounced. The main reason can be explained by the fact that the ECD technology has significantly reduced surface defects and residual stress in steel wires FeSi6.5, and, thus, increased the corrosion resistance. However, for steel wire 1070, the initial smooth surface and the microstructure of severe deformation were the dominant factors affecting the corrosion rate, and since the proportion of the positive effect that improves the corrosion resistance was reduced, there was therefore no obvious difference between the two technologies. Surface condition and internal stress were the main factors affecting the corrosion rate. ECD demonstrated an important effect on the promotion of plastic deformation and improvement of surface quality, and, therefore, was a promising technology for improving the formability of hard steels.

1. Introduction

For components serving in corrosive environments, corrosion induced by cold working cannot be ignored. After cold working, significant changes have occurred in both surface morphology and microstructure of the component, such as an increase of surface roughness, an increase of dislocation density, and refinement of grains. These changes affect not only the mechanical properties but also the corrosion resistance of the components. Robin et al. [1] reported that the corrosion resistance of cold-swaged and cold-drawn copper rods decreased in H_2SO_4 solution with the increase of the deformation degree, and cold drawing seemed to reduce the corrosion resistance more significantly than cold swaging under the same deformation condition. This phenomenon was attributed to a higher level of the stored energy induced by cold drawing. Hou et al. [2] showed that the corrosion resistance of both Ni-16Cr-15Mo and Ni-30Co-16Cr-15Mo alloys decreased after cold forging. Moreover, the corrosion resistance of the latter decreased more significantly compared to the former owing to its severely locally distorted lattice. Jinlong and Hongyun [3] found that the corrosion resistance of pure iron rolled at cryogenic temperature was lower than that of rolled at room temperature. The main reason was that the grain of the iron rolled at a cryogenic temperature has a higher dislocation density than the grain rolled at room temperature. The effect of the dislocation structure and dislocation density on the corrosion resistance of pure iron was larger than the effect of grain refinement or grain orientation. These results implied that work hardening induced by cold working could be one of the important factors in reducing the corrosion resistance of components.

The negative effect induced by work hardening may be reduced by applying anodic polarization to the component during processing. It was found for single cadmium and zinc crystals [4], copper [5], iron and steels [6-11], magnesium and aluminum alloys [9, 12] that a metal deformed plastically much more easily when it was exposed to a corrosive medium. For example, compared to the very low creep of die-cast Mg and Al alloys as well as stainless steel in air, these alloys showed a noticeable elongation and destruction in borate buffer solution and diluted sulfuric acid even at stresses of less than 70% of yield strength [9]. Recently, Gutman et al. [10] studied the effect of anodic polarization on surface hardness of AISI 1070 steel and FeSi6.5 steel. The results showed that the hardness of the anodically polarized sample significantly decreased in comparison with that in the air. Li et al. [13] found that the thicknesses of the deformation layers of both AM60B alloy and Mg_2Si_p/AM60B composite bars, drawn under anodic polarization condition, were thiner than that of the samples drawn in air.

In the present work, electrochemical cold drawing, when a sample is immersed in an electrolyte and anodically polarized when passing through a die plate, is used to produce hard steel wire (FeSi6.5 steel, AISI

DOI: 10.14456/jmmm.2019.28

1070 steel). The surface morphology, the mechanical characteristics and the corrosion behavior of hard steel wires, drawn by conventional CD technology and ECD method, were compared. It is found that enhanced corrosion resistance of wires obtain ed by ECD method is associated with an improvement in the surface conditions and a decrease in work hardening.

2. Materials and methods

Chemical compositions of AISI 1070 steel and FeSi6.5 steel are presented in Table 1. Hot-drawn wires with a diameter of 1.98 mm were cold drawn by CD and ECD technologies using a pilot drawing machine (Figure 1). Conventional cold drawing was carried out using emulsion and tap water as a lubricant, and the electrochemical cold drawing was carried out using 0.5 M H_2SO_4 solution as an electrolyte at anodic current densities of 5, 10 and 15 $mA \cdot cm^{-2}$. The parameters for CD and ECD methods are listed in Table 2. A pair of $12 \times 8 \times 1.5$ mm^3 copper sheets as the cathode were placed in the electrolyte cell symmetrically on both sides of the sample, which was anodiclly polarized in a sulphuric acid solution as it passed through the die. The drawing speed was 0.4 $m \cdot min^{-1}$. The drawing force was recorded using a force sensor. Before cold drawing, the oxide layer on the surface was removed with silicon carbide abrasive paper. After drawing, the wires were immediately cleaned with tap water and then dried with hot air.

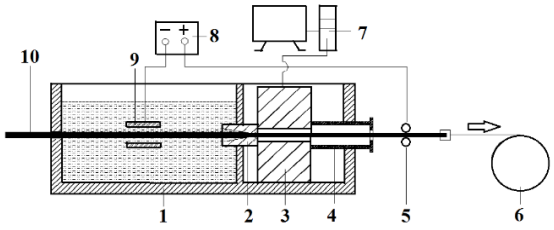

Figure 1. The ECD pilot device 1 - electrolyte cell (bath), 2 - drawing die, 3 - pressure sensor, 4 - pipe jacking, 5 - rollers (anode), 6 - drawing machine, 7 - computer, 8 - DC power supply, 9 - copper sheets (cathode), and 10 - hot-drawn wire.

The study of the electrochemical behavior of cold-drawn wires in 0.1 M HCl + 0.6M NaCl was carried out on 24 samples 5 cm long. This electrolyte is much less aggressive than 0.5 M H_2SO_4, and it was used to compare the corrosion resistance of wires obtained by the CD and ECD methods, depending on the technological parameters of wire drawing. Before being tested, 1070 wires were subjected to grinding with SiC paper (grade 320, 600 and 1200), then degreased and cleaned using the above-mentioned procedure. Wires FeSi6.5 were prepared by the same procedure, except for grinding, in which only a very thin layer was removed using 800 and 1200 graded SiC papers.

Table 1. Chemical composition (wt.%) of steels.

Material	C	Mn	Si	S	P	Fe
AISI 1070	0.72	0.78	0.24	0.042	0.032	balance
FeSi6.5	0.004	<0.1	6.5	0.003	0.004	balance

Table. 2. Parameters of wire cold drawing using the CD and ECD methods.

No.	Material	Diameter, mm	Treatment	Medium	i, $mA \cdot cm^{-2}$
1	AISI 1070	1.98	-	-	-
2		1.85	CD	regular emulsion	-
3		1.85	CD	water	-
4		1.87	ECD	0.5 M H_2SO_4	5
5		1.87	ECD	0.5 M H_2SO_4	10
6		1.87	ECD	0.5 M H_2SO_4	15
7	FeSi6.5	1.98	-	-	-
8		1.85	CD	regular emulsion	-
9		1.85	CD	water	-
10		1.85	ECD	0.5 M H_2SO_4	5
11		1.85	ECD	0.5 M H_2SO_4	10
12		1.85	ECD	0.5 M H_2SO_4	15

The corrosion studies for wires were conducted with the area S, exposed in the electrolyte, which was about 0.6 cm^2 (approximately 1.0 cm in length). The remaining surface of the wire, immersed in an electrolyte, was protected with epoxy resin, including the end of the sample, to prevent uncontrolled corrosion. After a potentiodynamic test, the protective epoxy resin was removed, and the actual corrosion area of the wires (S_a) was estimated using an average of 15-20 measurements of the length of the corroded surface, conducted by a microscope with a low magnification with a standard deviations of ± 0.1 mm. The corrosion test parameters of the wires were identical to those given above for the sheets. The potential of the working electrode with respect to the open circuit potential (OCP) ranged from -1.5 to +2.0 V_{SCE} with a sweep rate of 0.5 $mV \cdot s^{-1}$ for both the sheet samples and the wires. The working electrode was immersed in the solution for 15 min before measurement in order to reach a steady state and fix the potential of an open circuit.

The surface microhardness was measured on a Nano Indenter XP. The macroscopic characteristics of the samples surface were observed using an Ernst Leitz Wetzlar optical microscopy (OM). A Zeiss Supra 55 scanning electron microscope (SEM) was used to study the surface morphology and microstructure of the samples. The SEM equipped with an electron backscattered diffraction (EBSD) technique was carried out to determine elastic strains using samples cut in a longitudinal section parallel to the direction of wire drawing. The distance from the observation surface to the axis is four-fifths of the wire radius. The samples were polished by SiC papers and polishing paste with a particle size of 1.5 μm. The etching solution is 5% solution of nitric acid in pure water. Due to severe grain fragmentation, and differences in grain size and orientation distributions under CD and ECD technologies, there was a certain deviation in the statistics of grain size and misorientation angle distribution.

3. Results and discussion

For estimation of corrosion resistance of FeSi6.5 wires obtained by the CD and ECD processes, a very thin oxidation layer on the wire surface was removed by grinding prior to the corrosion tests. The heterogeneity of the surface made of carbon steel is much lower than that of silicon steel. The surface morphology of the initial AISI 1070 steel wires exhibits a typical cold drawing characteristic with a smooth surface, while that of the FeSi6.5 wires shows the hot drawing features with many pits, as shown in Figure 2. After cold drawing, the surface of the FeSi6.5 wires obtained by the CD method shows longitudinal scratches, while during electrochemical drawing this defect is less pronounced (Figure 3). However, the internal state of both 1070 and FeSi6.5 wires is characterized by typical fibrous microstructure with severe deformation obtained after cold drawing (Figure 4). Since the duration of the wire in the electrolyte (inlet wire) does not exceed several seconds, the weight loss due to corrosion will be insignificant. In our experiments, for example, in 0.3 molar sulfuric acid and current density of 5 mA cm^{-2}, the weight loss of a 2 mm in diameter 1070 wire does not exceed 0.2%.

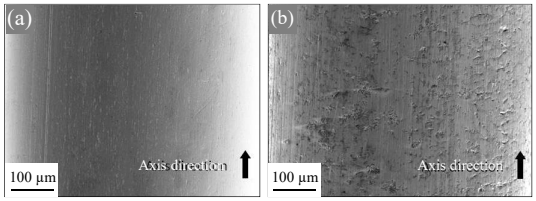

Figure 2. SEM photographs of surface morphology of the initial hot drawn wires 1070 (a) and FeSi6.5 (b).

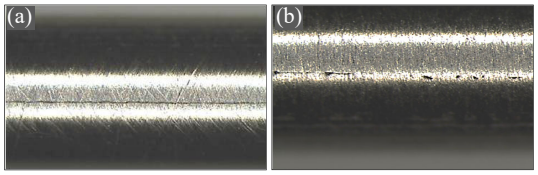

Figure 3. The longitudinal scratches in FeSi6.5 wires drawn by CD (a) and ECD (b) processes.

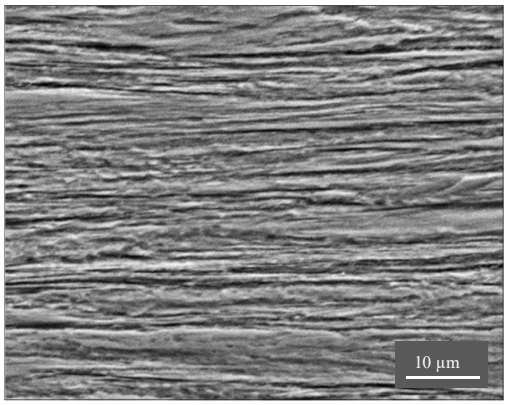

Figure 4. Microstructure of 1070 steel wire obtained by the ECD method.

The FeSi6.5 alloy is very hard and can hardly be drawn by the usual CD method at room temperature without surface defects. It is mainly due to the ordering structures [14]. As shown in Figure 5, for FeSi6.5 steel, a drawing force of 2600 N is needed to reduce the wire diameter from 1.9 to 1.85 mm using CD process, while only 1800 N drawing force for the AISI 1070 steel. The drawing force for the FeSi6.5 and 1070 steel wires under ECD condition is about 1800 N and 1200 N, respectively, which is 800 N (-31%) and 600 N (-33%) less than those under CD conditions. Drawing force is the resultant force of compressive force and friction force. Therefore, the friction force on the wires surfaces under ECD condition is smaller

than that under CD condition, which will produce fewer surface defects.

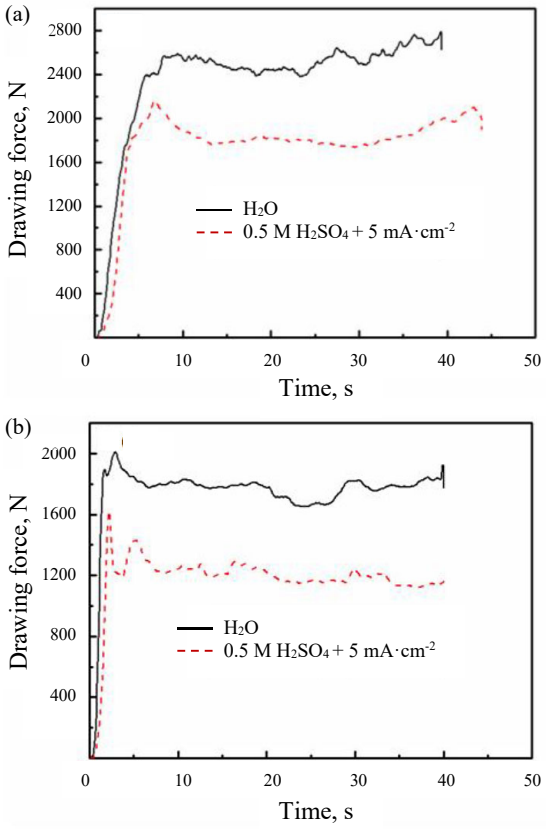

Figure 5. The drawing force to reduce wires diameter from 1.90 to 1.85mm using CD and ECD process, (a) FeSi6.5 steel; (b) AISI 1070 steel.

After reducing the area by 12.7%, which corresponds to a decrease in the wire diameter from 1.98 to 1.85 mm, the wires retain the original morphological surface characteristics. The average surface hardness of the wires FeSi6.5, obtained by CD and ECD technologies, at a current density of 0 (CD); 5 and 10 $mA \cdot cm^{-2}$ (ECD) is 6.54 GPa; 6.23 and 6.10 GPa, respectively. The result is consistent with the reduction of drawing force under anodic polarization (Figure 5a). The soften effect induced by the anodic polarization may result from a destruction of planar piles-ups dislocation near surface layer. The vacancies generated on the surface during anodic dissolution diffused into the metal and caused dislocation climb and an easier slip [5]. Gutman [7] suggested that the dissolution process may inject defects (vacancies, divacancies, or dislocations) into the metal lattice that affect plastic deformation.

The relative deformation between neighbor sites can be calculated by cross-correlation based analysis of EBSD patterns [15,16]. This technique involves capturing EBSD patterns from multiple locations on the sample, typically in a line scan or rectangular map, and then analyzing differences between the patterns to calculate the relative deformations between them. As shown in the EBSD strain contour micrograph (Figure 6) for FeSi6.5 wires, the ECD wire demonstrates significantly lower values of internal elastic strains compared to conventional drawing technology. The decrease in internal residual strains (and stresses) in the bulk of samples, detected by EBSD analysis, also corresponds to the same effect in the surface area, exposed to the corrosive solution. As is known from the literature, residual stress, induced, e.g., by cold working, can reduce the corrosion resistance of components. In accordance with mechanochemical theory, a stressed solid (working electrode), dissolved in an electrolyte, changes its equilibrium electrode potential due to mechanical stress. A decrease in the equilibrium electrode potential corresponds to an increase in mechanochemical activity and a decrease in the corrosion resistance of a solid [7]. Li et al. [17] found that the internal residual stress in X80 steel increases the sensitivity to corrosion by changing the microstructure of the metal matrix. It was also confirmed that the corrosion losses increase if residual stresses are present in the sample of AZ31 Mg alloy [18]. However, in some cases, the application of an elastic static tensile stress to a X100 pipe steel sample subjected to a near-neutral pH NS4 solution, did not change the steady-state corrosion potential [19]. Additionally, the deformation leads to changes in the electric potential of the metal, which controls the rate of corrosion processes [7,20]. Besides, the corrosion rate of metal decreased with a decrease in surface roughness, as well as surface defects [21-24]. It can be concluded that a lower level of residual stress and an improved surface quality of the wires obtained by the ECD technology, compared with the CD process, are the reasons for the increased corrosion resistance of the wires made using electrochemical drawing.

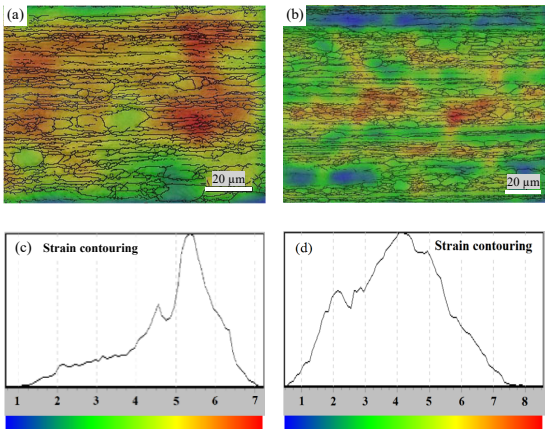

Figure 6. EBSD-strain contouring images of steel wire FeSi6.5 with a diameter of 1.85 mm, obtained using the CD (a and c) and ECD (b and d) processes.

Corrosion parameters, determined according to the Tafel law, a view of corroded area of wires, as well as corrosion diagrams for samples of sheets and wires,

are presented in Table 3 and Figures 7-9. The sheet samples for both steels presented approximately the same corrosion potential E_{corr} of about -490 mV_{SCE} in both solutions (Table 3, Figure 7). Silicon steel FeSi6.5 (6.5% Si) compared with carbon steel 1070 (0.24%Si) shows more than two times higher corrosion rates (22.4 and 10.2 mmpy), respectively, in a solution of 0.5 M H_2SO_4 and more than three times higher corrosion rates (1.3 and 0.4 mmpy) in 0.1 M HCl + 0.6 M NaCl solution, respectively (Table 3). Very similar values of Tafel's cathodic β_c and anodic β_a constants for both metals were found. For example, in sulfuric acid, the anodic Tafel slopes β_a are 58 mV and 67 mV for carbon steel and silicon steel, respectively while the cathodic Tafel slopes are 112 and 118, respectively. The less aggressive electrolyte containing hydrochloric acid demonstrates the β_c values 36 mV and 32 mV for 1070 steel and FeSi6.5, accordingly (Table 3). It is natural that the anode slope of the less aggressive second solution is almost half that of the former.

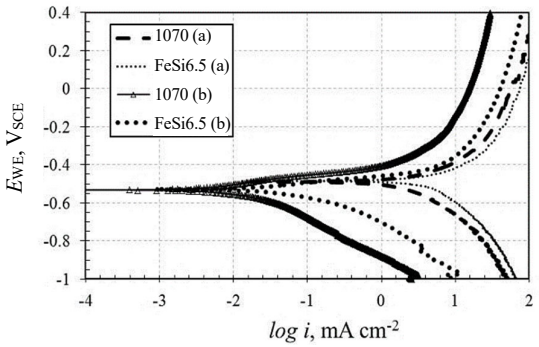

Figure 7. Potentiodynamic polarization curves obtained for sheet samples of steels 1070 and FeSi6.5 in 0.5 M H_2SO_4 (a) and 0.1 M HCl + 0.6 M NaCl (b) solutions.

After a potentiodynamic test of wires, as noted above, the length of the actual corrosion area of the wires 1070 and FeSi6.5 obtained using conventional drawing was estimated (Figure 8). During the test, the surface of the highly polished 1070 wires is close to uniform corrosion, although small pits are noted (Figure 8a). However, a noticeable deep scratch was observed in the corroded area of the FeSi6.5 wire (Figure 8b on the left), where anodic dissolution mainly occurs, while the non-corroded surface, protected from oxidation during the corrosion test, does not significant longitudinal defects (Figure 8b on the right).

The effect of the cold drawing technology on the corrosion parameters of FeSi6.5 wire is demonstrated in Figure 9 and 10, which show an increase in the corrosion resistance of the wire, performed by the ECD method compared to CD technology. This result is demonstrated by shifting the polarization curves for the "ECD" wires to the left (Figure 9), as well as by reducing the corrosion rate with increasing current density during the ECD process varying from 0 (CD) up to 15 mA·cm^{-2} (Figure 10). In Figure 9, the polarization curve corresponds to the wire obtained at 15 mA·cm^{-2} is not shown in the graph, since it overlaps with the curve for a current density of 10 mA cm^{-2}. As shown in Figure 10, the corrosion rate of the FeSi6.5 wires, obtained by the ECD method at various current densities, used during drawing, is 3.5-4 times (5 mA.cm^{-2}) and 1.7 times (10, 15 mA.cm^{-2}) lower than that of the wires FeSi6.5, obtained by the conventional CD method (i = 0). In a solution of 0.1 M HCl + 0.6 M NaCl, the corrosion potential of the working electrode Ewe demonstrates a noticeable positive shift equal to -460 mVSCE for the flat FeSi6.5 sample with excellent surface quality comparing to -690; -507 and -530 mVSCE for wires obtained by CD technology, as well as by the ECD method with i equal to 0, 10 and 15 mA·cm^{-2}, respectively (Figure 9).

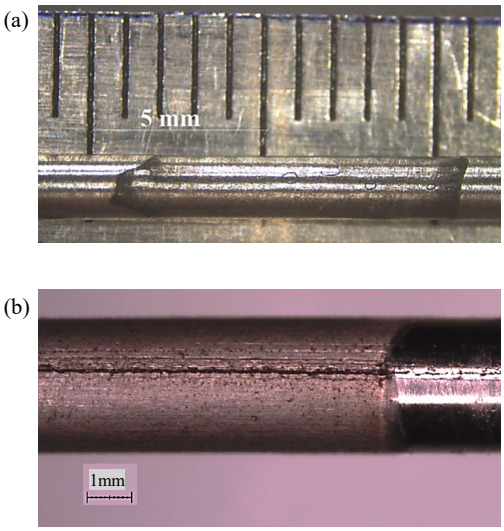

Figure 8. The corrosion area after a potentiodynamic testing for steel wires 1070 (a) and FeSi6.5 (b), obtained using the CD process.

Table 3. Corrosion potential, corrosion current density, Tafel's constants as well corrosion rate for the sheet samples.

Steel	Electrolyte	E_{corr}, mV	i_{corr}, µA·cm^{-2}	β_a, mV	β_c, mV	CR, mpy
AISI 1070	0.5 M H_2SO_4	-486	870	58	112	10.2
	0.1 M HCl + 0.6 M NaCl	-490	32	36	210	0.4
FeSi6.5	0.5 M H_2SO_4	-479	1,910	67	118	22.4
	0.1 M HCl + 0.6 M NaCl	-490	100	32	210	1.3

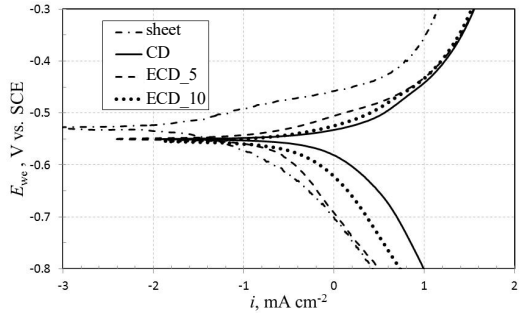

Figure 9. Potentiodynamic polarization curves for wires FeSi6.5, obtained at current densities 0 (CD), 5 and 15 mA·cm^{-2} (ECD), which were used in the pilot machine.

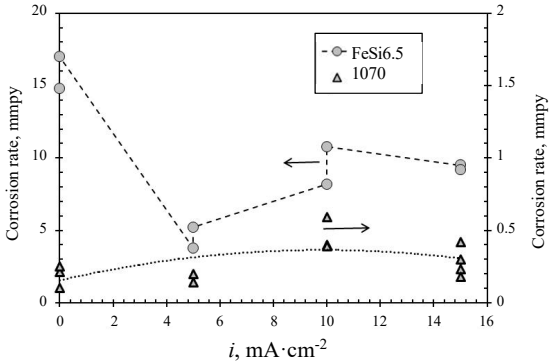

Figure 10. Effect of current density on the corrosion rate of 1070 and FeSi6.5 steel wires in 0.1 M HCl + 0.6 M NaCl solution obtained by the CD (i = 0) as well as by the ECD process.

Thus, a positive effect on the corrosion resistance of FeSi6.5 wires manufactured using ECD technology was found, compared to that obtained using the CD process. This can be explained by a decrease in the surface defects of these wires, obtained by the ECD technology, as compared with the conventional CD method (Figure 3). Compared to the smooth area, surface defects contain more active sites, where electrons more easily leave the matrix [23,24], which leads to an increase in the corrosion rate.

For AISI 1070 steel, it was found that the corrosion rates (CRs) in the HCl-based solution for both the mirror-polished sheet and the wire, were very close. For example, the CR value for the sheet sample was 0.40 mmpy (Table 3), and for the wires obtained by both processes it ranged from 0.28 to 0.48 mmpy (Figure 10). As shown in Figure 3, the 1070 steel wire presents the typical characteristic in the cold drawing state with smooth surface and severe strain fibrous microstructures. These decreased the fraction of the positive effect which improve corrosion resistance. It is shown [25] that the corrosion resistance of cold-drawn pearlitic steel decreases with increasing strain to 0.8 then increases with strain up to 1.6 because at lower strain the determined factor of the corrosion resistance is the defect concentration but at higher strain values the dominant one is the cementite volume fraction per lamellar structure. Thus, the difference in corrosion resistance between ECD and CD was not obvious.

4. Conclusions

1. In samples of sheets polished to a mirrow finish, the net corrosion rate of silicon steel FeSi6.5 compared with carbon steel AISI 1070 more than two times higher (22.4 and 10.2 mmpy) in a solution of 0.5 M H_2SO_4, respectively, and more than 3 times higher (1.3 and 0.4 mmpy) in a solution of 0.1 M HCl + 0.6 M NaCl, respectively.

2. The drawing force under ECD condition is significantly lower than under CD condition thanks to CME, which reduces the deformation resistance and friction force, additionally improves the surface quality and diminishes the residual stress, and, thus, increases the corrosion resistance.

3. Plasticization of the surface due to CME leads to a significant reduction in the corrosion rate of the very hard FeSi6.5 wires, obtained in the ECD process, compared to that in the CD process.

4. The initial state of AISI 1070 steel, with a smooth surface and severe strain microstructure, makes the effect of ECD on corrosion resistance insignificant.

5. Acknowledgements

This work is financially supported by the National Natural Science Foundation of China (51471031, U1660115) and the State Key Laboratory for Advanced Metals and Materials (2016Z-17).

References

[1] A. Robin, G. A. S. Martinez, and P. A. Suzuki, "Effect of cold-working process on corrosion behavior of copper," *Materials & Design*, vol. 34, pp. 319-324, 2012.

[2] Y. Hou, Y. Li, C. Zhang, Y. Koizumi, and A. Chiba, "Effects of cold working on corrosion resistance of Co-modified Ni–16Cr–15Mo alloy in hydrofluoric acid solution," *Corrosion Science*, vol. 89, pp. 258-267, 2014.

[3] L. Jinlong and L. Hongyun, "The effects of cold rolling temperature on corrosion resistance of pure iron," *Applied Surface Science*, vol. 317, pp. 125-130, 2014.

[4] E. N. Andrade, "Surface effect and structure of single crystal wires," *Nature*, vol. 164, pp. 536-537, 1949.

[5] R. W. Revie and H. H. Uhlig, "Effect of applied potential and surface dissolution on the creep behavior of copper," *Acta Metallurgica*, vol. 22, pp. 619-627, 1974.

[6] H. H. Uhlig, "Effect of surface dissolution on plastic deformation of iron and steel," *Journal of the Electrochemical Society*, vol. 123, pp. 1699-1701, 1976.

[7] E. M. Gutman, "*Mechanochemistry of Solid Surfaces*," New Jersey: World Scientific Publishing, 1994.

[8] E. M. Gutman, Ya. B Unigovski, Z. Koren, and B. Borohov, "Electrochemically enhanced plasticity of steels," *Journal of Metals, Materials and Minerals*, vol. 22, pp. 137-140, 2012.

[9] Ya. B. Unigovski, E. M. Gutman, Z. Koren, T. Poryadkov, and H. Rosenson, "Corrosion creep of metals", *Journal of Physics: Conference Series, vol.* 98, pp. 1-6, 2008.

[10] E. M. Gutman, Ya. B. Unigovski, R. Shneck, F. Ye, and Y. Liang, "Electrochemically enhanced surface plasticity of steels, *Applied Surface Science*, vol. 388, pp. 49-56, 2016.

[11] H. Guo, B. Lu, and J. Luo, "Response of surface mechanical properties to electro-chemical dissolution determined by in situ nanoindentation technique," *Electrochemistry communications*, vol. 8, pp. 1092-1098, 2006.

[12] Q. Wan and D. J. Quesnel, "Effects of NaCl, pH, and potential on the static creep behavior of AA1100," *Metallurgical and Materials Trans-actions A*, vol. 44, pp. 1311-1319, 2013.

[13] L. L. Li, T. J. Chen, S. Q. Zhang, and F. Y. Yan, "Electrochemical cold drawing of in situ Mg2Sip/AM60B composite: A comparison with the AM60B alloy," Journal of Materials Processing Technology, vol. 240, pp. 33-41, 2017.

[14] H. Li, Y. F. Liang, W. Yang, F. Ye, J. P. Lin, and J. X. Xie, "Disordering induced work softening of Fe–6.5wt%Si alloy during warm deformation," *Materials Science and Engineering: A*, vol. 628, pp. 262-268, 2015.

[15] A. J. Wilkinson, "Measurement of elastic strains and small lattice rotations using electron back scatter diffraction," *Ultramicroscopy*, vol. 62, pp. 237-247, 1996.

[16] A. J. Wilkinson, G. Meaden, and D. J. Dingley, "High-resolution elastic strain measurement from electron backscatter diffraction patterns: new levels of sensitivity," *Ultramicroscopy*, vol. 106, pp. 307-313, 2006.

[17] X. Li, F. Xie, D. Wang, C. Xu, M. Wu, D. Sun, and J. Qi, "Effect of residual and external stress on corrosion behaviour of X80 pipeline steel in sulphate-reducing bacteria environment," *Engineering Failure Analysis*, vol. 91, pp. 275-290, 2018.

[18] T. Hosaka, S. Yoshihara, I. Amanina, and B. J. MacDonald, "Influence of Grain Refinement and Residual Stress on Corrosion Behavior of AZ31 Magnesium Alloy Processed by ECAP in RPMI-1640 Medium," *Procedia Engineering*, vol. 184, pp. 432-441, 2017.

[19] Xu L.Y., Cheng Y. F., "An experimental investigation of corrosion of X100 pipeline steel under uniaxial elastic stress in a near-neutral pH solution," *Corrosion Science*, vol. 59, pp. 103-109, 2012.

[20] B. I. Kolodii, "Theoretical investigation of the interaction of a deformed metal with a corrosion medium," *Materials Science*, vol. 36, pp. 884-891, 2000.

[21] T. Hong and M. Nagumo, "Roughness and pitting corrosion of 301STS," *Corrosion Science*, vol. 39, pp. 1665-1672, 1997.

[22] K. Sasaki and G. T. Burstein, "The generation of surface roughness during slurry erosion-corrosion and its effect on the pitting potential," *Corrosion Science*, vol. 38, pp. 2111-2120, 1996.

[23] S. M. Lee, W. G. Lee, Y. H. Kim, and H. Jang, "Surface roughness and the corrosion resistance of 21Cr ferritic stainless steel," *Corrosion Science*, vol. 63, pp. 404-409, 2012.

[24] W. Li and D.Y. Li, "Influence of surface morphology on corrosion and electronic behavior," *Acta Materialia*, vol. 54, pp. 445-452, 2006.

[25] S. Xiang, Y. He, W. Shi, X. Ji, Y. Tan, J. Liu, and R. G. Ballinger, "Chloride-induced corrosion behavior of cold-drawn pearlitic steel wires," *Corrosion Science*, vol. 141, pp. 221-229, 2018.